

# Structural Rearrangements Induced by Photoexcitation in a RbCoFe Prussian Blue Derivative\*\*

Christophe Cartier dit Moulin, Guillaume Champion, Jean-Daniel Cafun, Marie-Anne Arrio, and Anne Bleuzen\*

Systems that undergo a reversible and controlled change of their physical properties offer appealing perspectives for the elaboration of electronic devices. Evidence of a photomagnetic effect in a CoFe Prussian blue analogue was a milestone in this research area and showed that molecular excitation can induce long-range magnetic order.<sup>[1]</sup> In the face-centered cubic structure of the CoFe Prussian blue analogues of chemical formula  $M_xCo_4[Fe(CN)_6]_{(8+x)/3}\square_{(4-x)/3}\cdot nH_2O$ ,  $M^+$  is an alkali-metal cation and  $\square$  represents the intrinsic  $[Fe(CN)_6]$  vacancies. Both of them are randomly distributed in the solid. The Wyckoff positions 4a (0, 0, 0) are occupied by Fe ions or  $\square$ , and the 4b positions ( $1/2, 1/2, 1/2$ ) by Co ions.<sup>[2]</sup> The alkali metal cations are distributed in the tetrahedral sites.<sup>[2]</sup> Such compounds may display unusual photomagnetic properties owing to light-induced electron transfer accompanied by a spin change on Co:  $Co^{III}(\text{low spin})Fe^{II} \rightarrow Co^{II}(\text{high spin})Fe^{III}$ .<sup>[1,3]</sup> The oxidation and spin states of the metal ions in the ground and photoexcited states are now well characterized.<sup>[3,4]</sup> However, some questions remain about the arrange-

ment of the atoms in both states. The answer to these questions is crucial to understanding the switchable properties of this family of compounds and to be able to elaborate new systems with improved properties in a rational way.

In Prussian blue derivatives, the  $[Fe(CN)_6]$  entities are always stable and rigid, highly stabilized in octahedral symmetry with linear Fe–C–N linkages because of the strong ligand-to-metal  $\pi$  backdonation and the low-spin (LS) state of Fe, regardless of whether the oxidation state of Fe is +II or +III. The bond lengths are very close in both oxidation states: 1.92 and 1.94 Å, respectively.<sup>[4]</sup> In previous work, we used X-ray absorption spectroscopy (XAS) to determine the Co crystal-field parameter ( $10Dq$ ) in CoFe Prussian blue analogues. We showed that this parameter is very sensitive to the environment of the most flexible species, that is, the Co coordination polyhedron.<sup>[5]</sup> Herein, we use this original method to determine the Co crystal-field parameter in the metastable photoexcited state of the rubidium Prussian blue derivative of chemical formula  $Rb_{1.8}Co^{III}_{3.3}Co^{II}_{0.7}[Fe^{II}(CN)_6]_{3.27}\cdot 13H_2O$  (RbCoFe). This compound was chosen since it displays a pronounced photomagnetic effect.<sup>[6,7]</sup>

The ground state of RbCoFe is essentially composed of photomagnetic  $Co^{III}(LS)Fe^{II}$  pairs, in which the  $10Dq(Co^{III})$  value (2.4 eV) is in line with  $Co^{III}$  in an octahedral site with linear  $Co^{III}$ –NC linkages.<sup>[5]</sup> For the remaining  $Co^{II}(HS)$  species, the Co–ligand bonds are long (2.08 Å) compared with those of their  $Co^{III}$  counterparts (1.91 Å).<sup>[3,4]</sup> The particularly low  $10Dq(Co^{II})$  value (0.7 eV) was explained by a bent geometry of Co–NC linkages to fit into the cubic structure with a short cell parameter ( $(9.96 \pm 0.05)$  Å)<sup>[8]</sup> imposed by the short  $Co^{III}$ –ligand bonds of the majority species. The environments proposed for both Co species are shown in Figure 1.<sup>[5]</sup>

The Co  $L_3$  edge of the photoinduced metastable state RbCoFe\* is shown in Figure 2, where it is compared with the spectrum of RbCoFe before irradiation. Peaks A to D are the signatures of sixfold-coordinated  $Co^{II}(HS)$ .<sup>[3,9]</sup> An increase in the energy gap between these peaks (A and D) corresponds to an increase in  $10Dq(Co^{II})$ .<sup>[10]</sup> Peaks E to G at higher energy are the signatures of  $Co^{III}(LS)$ , also sixfold-coordinated.<sup>[3]</sup> The relative intensity change of the  $Co^{II}$  and  $Co^{III}$  peaks after irradiation is due to photoinduced  $Co^{III} \rightarrow Co^{II}$  transformation.<sup>[3]</sup> Simulation of the RbCoFe\* spectrum by using the ligand-field multiplet model<sup>[9,11,12]</sup> reproduces very well the experimental data (Figure 2). The best simulation is obtained for a linear combination of 95% of  $Co^{II}(HS)$  and 5% of  $Co^{III}(LS)$ . The  $10Dq(Co)$  values obtained by multiplet

[\*] J.-D. Cafun, Prof. A. Bleuzen  
Université Paris Sud  
UMR 8182 (ICMMO)  
Equipe de Chimie Inorganique  
91405 Orsay Cedex (France)  
Fax: (+33) 1-6917-3207  
E-mail: annebleuzen@icmo.u-psud.fr

and  
CNRS  
91405 Orsay Cedex (France)

Dr. C. Cartier dit Moulin, Dr. G. Champion  
Laboratoire de Chimie Inorganique et Matériaux Moléculaires  
UMR CNRS 7071

Université Pierre et Marie Curie  
Bât. F, 4, place Jussieu, 75252 Paris Cedex 05 (France)  
and

Laboratoire pour l'Utilisation du Rayonnement Electromagnétique  
UMR CNRS 130-CEA-MENRS  
Bât. 209D, Université Paris-Sud  
BP 34, 91898 Orsay Cedex (France)

Dr. M.-A. Arrio  
Institut de Minéralogie et de Physique des Milieux Condensés  
UMR CNRS 7590-IPGP  
Universités Paris 6 et 7  
4 place jussieu, 75252 Paris Cedex 05 (France)

[\*\*] This research was supported by the European Community (Grant ERBFMRXCT980181), the contract TMR/TOSS (FMRX-CT98-0199), and the CNRS (Programme Matériaux). We acknowledge Michele Zacchigna (Elettra-Italy, BACH beamline) for assistance with XAS measurements.

Supporting information for this article is available on the WWW under <http://www.angewandte.org> or from the author.

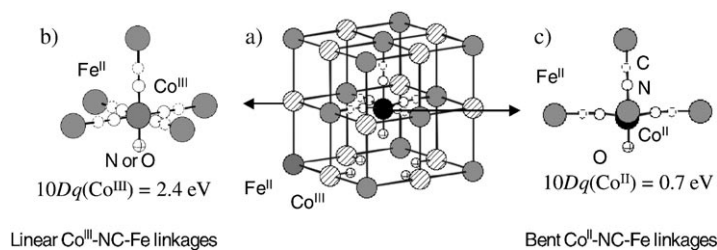


**Figure 1.** Scheme of a) a unit cell of  $\text{RbCoFe}$  containing both  $\text{Co}^{\text{III}}$  and  $\text{Co}^{\text{II}}$  species (alkali metal cations have been omitted for clarity) and proposed environments for b) the  $\text{Co}^{\text{III}}$  and c) the  $\text{Co}^{\text{II}}$  species forming the structure of the  $\text{RbCoFe}$  ground state.<sup>[5]</sup>

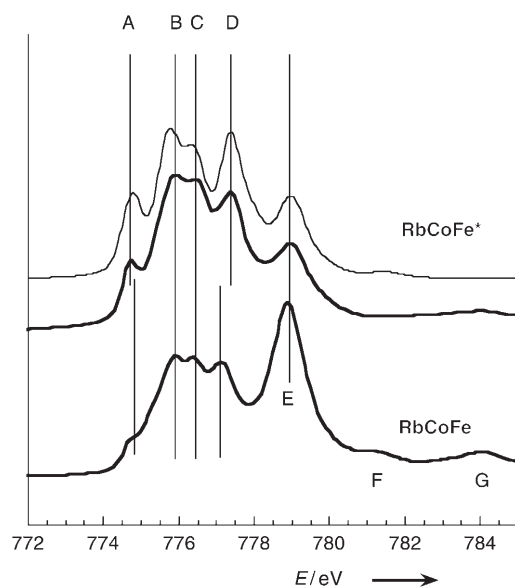


**Figure 2.** Experimental  $\text{Co L}_3$  edges of  $\text{RbCoFe}^*$  and  $\text{RbCoFe}$  (bold lines) and best simulation of the  $\text{RbCoFe}^*$  spectrum performed with the ligand-field multiplet model (normal line).

**Table 1:**  $10Dq(\text{Co})$  parameters given by multiplet calculation in the ground and photoinduced metastable states of  $\text{RbCoFe}$ .

	$10Dq$ [eV]	
	$\text{Co}^{\text{II}}(\text{HS})$	$\text{Co}^{\text{III}}(\text{LS})$
$\text{RbCoFe}$	0.7 <sup>[5]</sup>	2.4 <sup>[5]</sup>
$\text{RbCoFe}^*$	1.0	2.4

calculations are gathered in Table 1, where they are compared with the  $10Dq(\text{Co})$  value in  $\text{RbCoFe}$ .

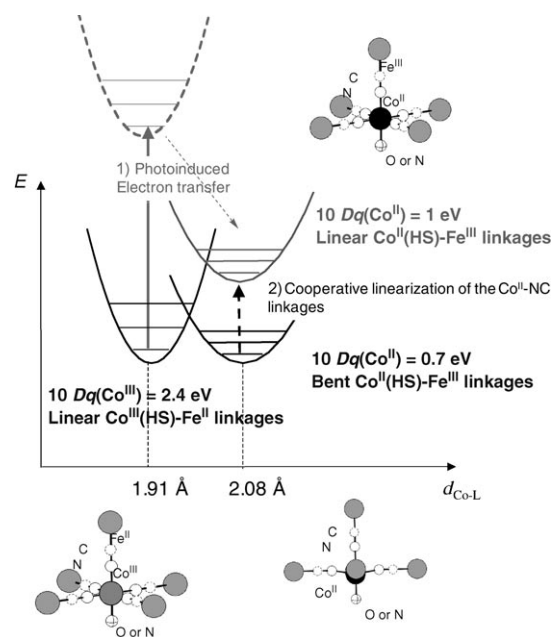
The  $10Dq(\text{Co}^{\text{III}})$  value after irradiation remains exactly the same as before irradiation (2.4 eV). Despite the pronounced increase in the cell parameter (from 9.96 Å to 10.28 Å)<sup>[8]</sup> and the change in oxidation state of most of the Co and Fe ions under irradiation, the 5% of remaining  $\text{Co}^{\text{III}}$  species are locally stabilized in a specific environment for which the  $10Dq(\text{Co}^{\text{III}})$  value is in line with linear  $\text{Co}^{\text{III}}\text{-NC-Fe}$  linkages.

The  $10Dq(\text{Co}^{\text{II}})$  value after irradiation is much higher than that of the ground state (1 eV compared to 0.7 eV), and it is in the expected spectral range for linear  $\text{Co}^{\text{II}}\text{-NC}$  linkages

with  $\pi$ -donor N-ligating CN bridges. It is comparable to the ligand field exerted by the  $\pi$ -donor N-ligating  $\text{NCS}^-$  anion and close to that exerted by  $\text{OH}_2$ .<sup>[5,13,14]</sup> Under irradiation  $\text{Co}^{\text{III}}$  species with linear  $\text{Co}^{\text{III}}\text{-NC-Fe}$  linkages would then be transformed into  $\text{Co}^{\text{II}}$  species also with linear  $\text{Co}^{\text{II}}\text{-NC-Fe}$  linkages.

Attempts to reproduce the spectrum of  $\text{RbCoFe}^*$  with the ground-state  $10Dq(\text{Co}^{\text{II}})$  value (0.7 eV) and an additional one related to the phototransformed  $\text{Co}^{\text{II}}$  failed. All the  $\text{Co}^{\text{II}}(\text{HS})$  with a  $10Dq(\text{Co}^{\text{II}})$  value of 0.7 eV, initially present in the ground state, are fully transformed into  $\text{Co}^{\text{II}}(\text{HS})$  with a  $10Dq(\text{Co}^{\text{II}})$  value of 1 eV. In the photoexcited state, the  $\text{Co}^{\text{II}}$  crystal field is independent of the chemical composition of the  $\text{Co}(\text{NC})_{(6-x)}(\text{OH}_2)_x$  coordination sphere, which may vary owing to the random distribution of the  $[\text{Fe}(\text{CN})_6]$  vacancies. The significant increase in  $10Dq(\text{Co}^{\text{II}})$  of the  $\text{Co}^{\text{II}}$  initially in the ground state is then necessarily related to cooperative structural effects.

An explanation for the  $10Dq(\text{Co})$  values found in the ground and excited metastable states of  $\text{RbCoFe}$  is sketched in Scheme 1. We propose associated environmental and



**Scheme 1.** Co species implicated in the photomagnetic effect: environment,  $10Dq(\text{Co})$  values, and associated potential wells (black for the ground state, gray for the metastable state).

electronic potential wells for the species implicated in the photomagnetic effect. In the ground state, both energetically low lying potential wells (in black in Scheme 1) are populated in correspondence to the  $\text{Co}^{\text{III}}$  majority species with linear linkages and the  $\text{Co}^{\text{II}}(\text{HS})$  species in strained environment. Under irradiation the  $\text{Co}^{\text{III}}$  species with linear linkages are photoexcited and trapped in a metastable state in which the  $\text{Co}^{\text{II}}$  species are also surrounded by linear linkages (gray potential well in Scheme 1). Cobalt–ligand bond lengthening and a significant increase in the cell parameter accompany the

photoinduced electron transfer. As the cell parameter increases, the strain imposed by the short lattice parameter on the  $\text{Co}^{\text{II}}(\text{HS})$  species initially present in the ground state relaxes and, as a consequence, the bent  $\text{Co}^{\text{II}}\text{--NC--Fe}$  linkages become linear.

For the first time, we have shown that the  $10Dq(\text{Co}^{\text{II}})$  value in the metastable  $\text{RbCoFe}^*$  state of the Prussian blue analogue is in line with  $\text{Co}^{\text{II}}$  species with linear  $\text{Co}^{\text{II}}\text{--NC--Fe}$  linkages as the  $\text{Co}^{\text{III}}$  species in the ground state. In that linear geometry, 1) the  $\text{Co}^{\text{III}}(\text{LS})\text{Fe}^{\text{II}}$  state is the ground state and 2) the  $\text{Co}^{\text{II}}(\text{HS})\text{Fe}^{\text{III}}$  metastable state would be sufficiently close in energy to be phototrapped with a long lifetime.

This study also clearly shows that, beyond the two  $\text{Co}^{\text{II}}\text{Fe}^{\text{III}}$  and  $\text{Co}^{\text{III}}\text{Fe}^{\text{II}}$  electronic states commonly evoked to describe the switchable properties of this family of compounds, different  $\text{Co}^{\text{II}}(\text{HS})\text{Fe}^{\text{III}}$  states are likely to exist in CoFe Prussian blue analogues. For a long time, the nonphotomagnetic  $\text{Co}^{\text{II}}_4[\text{Fe}^{\text{III}}(\text{CN})_6]_{12.7}\cdot 18\text{H}_2\text{O}$  (CoFe), which is free of alkali metal cations, has been taken as a reference for the  $\text{RbCoFe}^*$  photoexcited state. They are both mainly composed of  $\text{Co}^{\text{II}}(\text{HS})\text{Fe}^{\text{III}}$  with short  $\text{Co}^{\text{II}}\text{--ligand}$  bonds (2.08 Å at 10 K for  $\text{RbCoFe}^{*\text{[3]}}$  and 2.095 Å at 30 K for  $\text{CoFe}^{\text{[4]}}$ ). They also exhibit close cell parameters ((10.28 ± 0.05) Å at 10 K for  $\text{RbCoFe}^{*\text{[8]}}$  and (10.32 ± 0.05) Å at 300 K for  $\text{CoFe}^{\text{[4]}}$ ). However, we show herein that the  $10Dq(\text{Co}^{\text{II}})$  values in the two states are completely different. They reflect different geometries of the  $\text{Co--NC--Fe}$  linkages: bent in CoFe ( $10Dq(\text{Co}^{\text{II}}) = 0.55 \text{ eV}$ )<sup>[5]</sup> and linear in the  $\text{RbCoFe}^*$  photoexcited state (1 eV). These two different geometries obviously lead to different photomagnetic properties.

Work is in progress to chemically control the geometry of the  $\text{M}_1\text{--NC--M}_2$  linkages, since the switchable properties of these compounds seem to be strongly correlated to the geometry of the bridges.

### Experimental Section

The synthesis of  $\text{Rb}_{1.8}\text{Co}^{\text{III}}_{3.3}\text{Co}^{\text{II}}_{0.7}[\text{Fe}^{\text{II}}(\text{CN})_6]_{13.27}\cdot 13\text{H}_2\text{O}$  was described elsewhere.<sup>[7]</sup>

The  $\text{Co L}_{2,3}$  edges were collected at the Beamline for Advanced diCHroism (BACH)<sup>[15]</sup> at the ELETTRA Synchrotron Radiation Source in Trieste, Italy.

All the photomagnetic CoFe Prussian blue analogues are excited under the synchrotron X-ray beam. We checked that the  $\text{Co L}_3$  edge spectrum of  $\text{RbCoFe}^*$  is the same at 4 K when the compound has been photoexcited in the visible spectral range ((750 ± 50) nm) and photoexcited by the X-ray beam itself.

XAS data parameters of the calculated spectra and a brief description of the simulation method are available as Supporting Information.

Received: September 18, 2006

Published online: January 9, 2007

**Keywords:** crystal-field parameters · electron transfer · metastable states · Prussian blue analogues · X-ray absorption spectroscopy

- [1] O. Sato, T. Iyoda, A. Fujishima, K. Hashimoto, *Science* **1996**, 272, 704–705.
- [2] A. Lüdi, H. U. Güdel, *Structure and Bonding*, Springer, Berlin **1973**, pp. 1–21; H. J. Buser, D. Schwarzenbach, W. Peter, A. Lüdi, *Inorg. Chem.* **1977**, 16, 2704–2710.
- [3] C. Cartier dit Moulin, F. Villain, A. Bleuzen, M.-A. Arrio, P. Sainctavit, C. Lomenech, V. Escax, F. Baudalet, E. Dartyge, J. J. Gallet, M. Verdaguer, *J. Am. Chem. Soc.* **2000**, 122, 6653–6658.
- [4] T. Yokoyama, T. Ohta, O. Sato, K. Hashimoto, *Phys. Rev. B* **1998**, 58, 8257–8266.
- [5] a) V. Escax, G. Champion, M.-A. Arrio, M. Zacchigna, C. Cartier dit Moulin, A. Bleuzen, *Angew. Chem.* **2005**, 117, 4876–4879; *Angew. Chem. Int. Ed.* **2005**, 44, 4798–4801; b) V. Escax, G. Champion, C. Cartier dit Moulin, A. Bleuzen, M.-A. Arrio, M. Zacchigna, M. Zangrando, F. Bondino, *Elettra Highlights* **2005**, 14–16.
- [6] A. Goujon, O. Roubeau, F. Varret, A. Dolbecq, A. Bleuzen, M. Verdaguer, *Eur. Phys. J. B* **2000**, 14, 115–124.
- [7] A. Bleuzen, C. Lomenech, V. Escax, F. Villain, F. Varret, C. Cartier dit Moulin, M. Verdaguer, *J. Am. Chem. Soc.* **2000**, 122, 6648–6652.
- [8] V. Escax, A. Bleuzen, J. P. Itié, P. Münsch, F. Varret, M. Verdaguer, *J. Phys. Chem. B* **2003**, 107, 4763–4767.
- [9] M. A. Arrio, P. Sainctavit, C. Cartier dit Moulin, T. Mallah, M. Verdaguer, E. Pellegrin, C. T. Chen, *J. Am. Chem. Soc.* **1996**, 118, 6422–6427.
- [10] G. van der Laan, I. W. Kirkman, *J. Phys. Condens. Matter* **1992**, 4, 4189–4204.
- [11] R. Cowan, *The Theory of Atomic Structure and Spectra*, University of California Press, Berkeley, **1981**.
- [12] P. Butler, *Point Group Symmetry—Methods and Tables*, Plenum Press, New York, **1981**.
- [13] C. K. Jorgensen, *Modern Aspect of Ligand Field Theory*, North-Holland, Amsterdam, **1971**.
- [14] A. Lever, *Inorganic Electronic Spectroscopy*, 2nd ed., Elsevier, Amsterdam, **1984**.
- [15] M. Zangrando, M. Finazzi, G. Paolucci, G. Comelli, B. Diviacco, R. P. Walker, D. Cocco, F. Parmigiani, *Rev. Sci. Instrum.* **2001**, 72, 1313–1316.